Published in final edited form as:

Nat Mater. 2018 June ; 17(6): 528–534. doi:10.1038/s41563-018-0028-2.

A facile approach to enhance antigen response for personalized cancer vaccination

Aileen Weiwei Li[1,2], **Miguel C. Sobral**[1,2], **Soumya Badrinath**[3], **Youngjin Choi**[4], **Amanda Graveline**[2], **Alexander G. Stafford**[2], **James C. Weaver**[2], **Maxence O. Dellacherie**[1,2], **Ting-Yu Shih**[1,2], **Omar A. Ali**[2], **Jaeyun Kim**[4,5,6], **Kai W. Wucherpfennig**[3], and **David J. Mooney**[1,2]

[1]John A Paulson School of Engineering and Applied Sciences, Harvard University, Cambridge, MA, USA

[2]Wyss Institute for Biologically Inspired Engineering, Harvard University, Boston, MA, USA

[3]Department of Cancer Immunology and Virology, Dana-Farber Cancer Institute, Boston, MA, USA

[4]School of Chemical Engineering, Sungkyunkwan University, Suwon 16419, Republic of Korea

[5]Department of Health Sciences and Technology, Samsung Advanced Institute for Health Science & Technology (SAIHST), Sungkyunkwan University, Suwon 16419, Republic of Korea

[6]Biomedical Institute for Convergence at SKKU (BICS), Sungkyunkwan University, Suwon 16419, Republic of Korea

Abstract

Existing strategies to enhance peptide immunogenicity for cancer vaccination generally require direct peptide alteration, which beyond practical issues may impact peptide presentation and result in vaccine variability. Here, we report a simple adsorption approach using polyethyleneimine (PEI) in a mesoporous silica micro-rod (MSR) vaccine to enhance antigen immunogenicity. The MSR-PEI vaccine significantly enhanced host dendritic cell activation and T cell response over the existing MSR vaccine and bolus vaccine formulations. Impressively, a single injection of the MSR-PEI vaccine using an E7 peptide completely eradicated large established TC-1 tumors in ~80% of mice and generated immunological memory. When immunized with a pool of B16F10 or CT26 neoantigens, the MSR-PEI vaccine eradicated established lung metastases, controlled tumor growth and synergized with anti-CTLA4 therapy. Our findings using three independent tumor

Correspondence should be addressed to D.J.M. (mooneyd@seas.harvard.edu).

Author Contributions:
A.W.L and D.J.M conceived the study, designed the experiments and wrote the manuscript, A.W.L, M.C.S, S.B, Y.C, A.G, A.G.S, J.C.W, M.O.D and T-Y.S performed the experiments. S.B. and K.W.W. designed and performed the TIL experiments. Y.C and J.K designed and performed the TEM and MSR pore analysis experiments. O.A.A contributed to the study design.

Competing Financial Interests:
The authors declare no competing financial interests.

Data Availability Statement:
The datasets generated during and/or analyzed during the current study are available from the corresponding author on reasonable request.

models suggest that the MSR-PEI vaccine approach may serve as a facile and powerful multi-antigen platform to enable robust personalized cancer vaccination.

Keywords

cancer immunotherapy; personalized vaccine; neoantigen; mesoporous silica; polyethyleneimine

Cancer vaccines targeting multiple tumor specific antigens can elicit broad immune responses and decrease tumor escape[1,2], and recent advances enable identification of tumor specific mutations ("neoantigens")[3,4]. Neoantigens are attractive vaccine targets as they are not expressed in healthy tissues and are predicted to have strong MHC binding affinity[5]. Recent clinical data showed that neoantigen vaccines could generate T cells specifically targeting heterogeneous tumor clones[6]. However, neoantigen peptides exhibit rapid clearance and low immunogenicity, which limits optimal presentation by antigen presenting cells (APCs) to initiate strong T cell responses[7]. Macro- and nano-engineering strategies have been designed to overcome these challenges[8–11], but many approaches require chemical modification or physical emulsification of the peptides, potentially altering their presentation capacity. Moreover, since neoantigen vaccines typically require many peptides[12], modification of individual peptides is cumbersome for clinical translation and likely results in high batch-to-batch variability.

We propose a facile strategy to enhance antigen immunogenicity using polyethyleneimine (PEI) combined with a mesoporous silica micro-rod (MSR) vaccine. The MSR vaccine can be injected using standard needles, was shown to effectively concentrate and activate large populations of host APCs, and induced more potent humoral responses and prophylactic tumor protection than traditional vaccine formulations[13]. Moreover, the MSR surface could potentially be modified to induce stronger responses. Recent studies have shown that complexes based on PEI, a widely used cationic polymer[14,15], can stimulate pro-inflammatory cytokine production[16,17], and induce potent humoral responses when complexed with glycoproteins[18]. Here, we explore the application of PEI to co-present antigen in a facile, layered adsorption manner in the MSR vaccine.

MSRs were adsorbed with PEI (MSR-PEI) by simply mixing with a PEI solution for 15 minutes; subsequently, an antigen pool was directly adsorbed onto MSR-PEI particles (Fig 1a). Both 60K branched PEI (B60K) and 25K linear PEI (L25K) absorbed to MSR with high efficiency (Fig. 1b), with an incorporation capacity of ~20ug PEI/mg MSR. Over 90% of B60K and L25K PEI polymers were adsorbed after 1 minute of mixing (Fig 1c). Zeta potential measurements confirmed PEI incorporation (Fig 1d). MSR-PEIs maintained the intrinsic mesopores of MSRs (Supplementary Fig 1a), pore structure and bulk particle structure (Supplementary Fig 1b–d), with reduced surface area and pore volume as expected (Supplementary Table 1). MSRs and MSR-PEIs showed high incorporation efficiency for net positive and neutral example murine (Fig 1e) and human (Fig 1f) peptides, but MSR-PEI enhanced the incorporation of net negative peptides.

The underlying adjuvant effect of PEI[19,20] on bone marrow derived dendritic cells (BMDCs) was next examined. BMDCs take up free PEI, reaching maximum uptake at 24 hours

(Supplementary Fig 2a), and showed a significant increase in CD86 and MHC-II expression (Fig 1f), and TNFα (Fig 1g) and IL-6 (Fig 1h) production in a PEI dose dependent manner. BMDCs stimulated with MSR-PEI also showed significantly increased CD86 expression (Supplementary Fig 2b) and TNFα production (Supplementary Fig 2c). MSR-PEI also triggered the increased production of IL-1β, a key cytokine produced in response to Nlrp3 inflammasome activation[21] (Supplementary Fig 3a). This was likely a result of lysosomal rupture upon MSR-PEI uptake (Supplementary Fig 3b), leading to the release of phagosomal contents into the cytosolic compartment. Interestingly, as TNFα and IL-6 have been shown to be Nlrp3-independent cytokines[22], it is possible that MSR-PEI particles can stimulate multiple damage-associated molecular patterns (DAMP) receptors. The impact of PEI on antigen presentation was next examined by pulsing BMDCs with ovalbumin (OVA) either alone or together with B60K PEI for 2 days. B60K PEI led to ~10–20× increase in antigen cross-presentation compared to OVA alone (Fig 1i). Finally, as the MSRs and PEI solutions were endotoxin free (Supplementary Table 2), and BMDC activation was unaffected by TLR4 neutralization (Supplementary Fig 4), the activation of DCs was unlikely a result of material contamination. Together, these data suggest PEI can be efficiently and easily incorporated into MSRs, a broad range of neoantigen peptides can be subsequently incorporated via adsorption, and PEI and MSR-PEI particles can enhance DC activation and cross-presentation.

The ability of an MSR-PEI vaccine to improve DC activation *in vivo* was then analyzed by comparing the MSR vaccine incorporating GM-CSF to recruit host DCs, the TLR-9 agonist CpG-ODN and a model antigen OVA as previously described[13] to the MSR-PEI vaccine incorporating these agents (Fig 2a). *In vitro*, GM-CSF and PEI were released in a sustained manner from the MSR-PEI vaccine, while CpG was rapidly released due to its negative charge (Supplementary Fig 5). Mice were immunized with the MSR vaccine (V) or the MSR-PEI vaccine (VP). In both vaccines, CpG-ODN was incorporated as TLR-9 activation can efficiently induce a type 1 and CTL response[23]. The total number of cells recruited to the vaccine on day 3 was comparable between V and VP immunized mice (Fig 2b). However, VP showed a significant enrichment of $CD11c^{+}CD86^{+}$ activated DCs (Fig 2c), $CD11c^{+}CCR7^{+}$ LN homing DCs (Fig 2d) and $CD11c^{+}$SIINFEKL-$H2K^{b+}$ antigen cross-presenting DCs (Fig 2e). The vaccine draining lymph node (dLN) total cellularity between V and VP immunized mice was similar on day 3, but VP immunized mice showed strikingly higher dLN cellularity on day 5 (Fig 2f). Additionally, VP elicited a strong enrichment in activated DCs (Fig 2g and Supplementary Fig 6a) and antigen presenting DCs (Fig 2h), but not in the macrophage populations (Supplementary Fig 6b,c) in the dLN. Next, the impact of a direct association between antigen and PEI was evaluated. While maintaining a constant dose of GM-CSF, CpG, OVA and PEI, two types of VP vaccines were tested: 1. A trans form (trans VP) that combined CpG adsorbed onto MSR-PEIs, OVA adsorbed onto bare MSRs and GM-CSF adsorbed onto also bare MSRs, or 2. A cis form (cis VP) that combined OVA adsorbed onto MSR-PEIs, CpG adsorbed on to bare MSRs and GM-CSF adsorbed onto also bare MSRs (Fig 2i). The incorporation efficiencies of GM-CSF, CpG and OVA were comparable (Supplementary Table 3). The cis VP vaccine showed 2× more activated DCs in the scaffold (Fig 2j) and 3× more activated and antigen-presenting DCs in the dLN (Fig 2k,l) compared to the trans VP vaccine. The myeloid cell population in the scaffold was not

impacted (Supplementary Fig 6d). Collectively, these data demonstrate that the MSR-PEI vaccine enhanced host DC activation, antigen presentation and trafficking to secondary lymphoid organs.

The ability of the MSR-PEI vaccine to induce a CD8 killer T cell (CTL) response with a model antigen OVA was next examined. Circulating blood PBMCs were analyzed 7 days after immunization with V or VP vaccines. Mice immunized with VP generated ~2× higher circulating IFNγ^+ (Fig 3a) and tetramer$^+$ (Fig 3b) CTLs compared to V. Furthermore, effector T cells outnumbered regulatory T cells by ~15× at the VP vaccine site, almost 3 times higher than the V vaccine site (Fig 3c). Increasing the PEI dose in VP to above 40ug/vaccine led to a decrease in CTL responses (Fig 3d). Similarly to VP using B60K PEI, the VP formulation using L25K PEI also showed an enhanced CTL response compared to V (Fig 3e). No significant differences were observed when varying PEI structure and molecular weight (Supplementary Fig 7a). Finally, and consistent with our previous finding on host DC activity, a cis VP vaccine showed a significantly higher CTL response compared to a trans VP vaccine and the MSR vaccine (Fig 3f). To exclude the possibility that a higher dose of PEI in the trans VP vaccine may improve the response, two increasing doses of PEI in the trans VP vaccine were evaluated and the CTL response decreased with increasing PEI (Supplementary Fig 7b).

To test whether the MSR-PEI vaccine may induce anti-tumor immunity against tumor specific peptides, a synthetic long peptide derived from the E7 oncoprotein of human papilloma virus (HPV) was used as the antigen. Beyond cervical cancer, HPV is associated with 30–60% of oropharyngeal, vaginal and head-and-neck cancers[24–26]. Consistent with our findings using OVA antigen, VP induced ~2–3× higher E7 specific IFNγ^+ (Fig 4a) and tetramer$^+$ (Fig 4b) circulating CTLs compared to V. Mice immunized with VP showed a significantly elevated blood TNFα levels (Fig 4c). Next, mice were inoculated with E7 expressing TC-1 carcinoma subcutaneously and treated with a single injection of V or VP when tumor areas reached ~25 mm. VP triggered rapid and complete regression in a majority of the animals, whereas the V induced only partial regression (Fig 4d). Importantly, VP led to complete regression of even tumors that reached large dimensions (~1×1cm). VP also enhanced overall survival by ~2× compared to V. Impressively, ~80% of animals treated with VP survived long term beyond 150 days (Fig 4e). To test immunological memory, the animals that survived from the first inoculation were re-challenged with the same E7 expressing TC-1 carcinoma after 6 months. All mice that were treated with either V or VP, and survived the first tumor inoculation, were completely tumor free after the re-challenge (Fig 4e). In a separate experiment, VP was evaluated against a traditionally formulated bolus vaccine. Consistent with previously reported findings, the bolus vaccine was partially effective and induced complete regression in only ~20% of the animals[9,26]. In comparison, VP induced faster regression and ~80% of treated animals again showed complete regression (Supplementary Fig 8a and 8b). The anti-tumor effect of VP was antigen specific (Fig 4f) and mediated by CD8$^+$ T cells (Fig 4g,h). Importantly, the therapeutic regression accomplished with just one immunization with VP was stronger than multiple treatments of conventionally adjuvanted E7 vaccines, and mRNA and nanoparticle-based technologies in similar tumor studies[27,9,28,29]. To further demonstrate that a direct association between the antigen and PEI in the vaccine is important, animals bearing established subcutaneous TC-1

tumors were treated with trans VP (E7 VP trans), and cis VP (E7 VP cis). Mice treated with cis VP showed superior tumor regression (Supplementary Fig 8c), indicating that co-presentation of the antigens and PEI in the vaccine is likely a crucial component to generating anti-tumor immunity.

Finally, the MSR-PEI vaccine's ability to serve as a facile and effective platform for multiple neoantigens to induce tumor control was tested. First, VP demonstrated superior CTL response against B16F10 neoantigens in both tumor-free and tumor-bearing mice compared to V (Supplementary Fig 9,10). Next, VP was evaluated in the highly aggressive and immune-suppressive B16F10 and CT26 models using combinations of neoantigen peptides[5]. As effector tumor infiltrating lymphocytes (TILs) are needed to achieve tumor clearance[7], the TIL population was isolated, directly stained and analyzed on day 15 after inoculation, by which point some tumors in the untreated and V-treated animals had developed to the maximum allowed size. Impressively, tumors in VP-treated animals showed stronger enrichment in the IFNγ^+, TNFα^+ and Granzyme B$^+$ TILs (Fig 5a, Supplementary Fig 11). In contrast, V did not generate enhanced TIL response compared to untreated animals. Lung metastases of B16F10 (Fig 5b) and CT26 (Supplementary Fig 12) tumors were efficiently eradicated by one injection of VP containing a combination of B16 or CT26 neoantigens, respectively. Notably, these responses achieved with a single immunization of VP were comparable to those achieved with repeated immunizations of RNA-based neoantigen vaccines[5]. A standard prime and boost of VP improved subcutaneous B16F10 growth control (Fig 5c) and induced temporary regression in a subset of the animals (Fig 5d). Checkpoint blockade therapies are effective in various types of cancer, but the response rate depends on a preexisting immunity[30]. In this aggressive model, anti-CTLA4 therapy alone did not confer significant tumor growth control. However, one injection of VP in combination with anti-CTLA4 treatment significantly augmented the response (Fig 5e).

This study describes a potentially transformative, simple and modular strategy to enhance antigen immunogenicity and drive effective anti-tumor immunity. This approach can effectively drive immune responses against libraries of cancer specific mutations and synergize with other immunotherapies. The vaccine is assembled in less than three hours by simple mixing of all components, and can be stored in lyophilized form before or after antigens are added. Overall, this approach may have strong value as a therapeutic multi-antigen platform to enable robust personalized vaccination.

Methods

Materials, cell line and peptides

Branched 60K PEI (Sigma 181978), Branched 2K PEI (Polysciences 06089), Linear 25K PEI (Polysciences 23966) and Linear 2K PEI (Polyscienes 24313) were diluted to 5.5mg/ml in PBS, pH'ed to 7.4 and stored away from direct light. Endotoxin free ovalbumin (OVA) was used throughout the study (Invivogen, vac-pova). OVA was diluted to 5mg/ml in endotoxin free water. All antibodies were used according to the manufacturer's protocols. SIINFEKL- and $E7_{49–57}$-tetramers were obtained from the Emory NIH Tetramer Core Facility. TC-1 cells were generated in the laboratory of T-C. Wu (Johns Hopkins University, Baltimore, USA, tested to be mycoplasma-free) and maintained in RPMI supplemented with

10% FBS, 1% penicillin–streptomycin and 50ug/ml G418[24]. B16F10 (ATCC) and CT26 cells (ATCC) were maintained in DMEM supplemented with 10% FBS and 1% penicillin–streptomycin according to protocols from ATCC. Peptides used in this study are listed in Supplementary Table 4. All murine peptides used in this study were synthesized at least 95% purity from Peptide 2.0. All human neoantigen peptides were provided by Dr. Catherine J Wu (Dana Farber Cancer Institute, Harvard Medical School, USA). Peptides were first dissolved in DMSO to 50 mg/ml and further diluted in endotoxin free water. Flow cytometry antibodies used in this study are listed in Supplementary Table 5.

Vaccine formulations

MSRs were synthesized as described previously[13]. All vaccine components were incorporated after the MSRs were synthesized.

To formulate the MSR-PEI or cis MSR-PEI vaccine, 2mg of the MSR (50mg/ml working solution in PBS) were adsorbed with 100ug murine class B CpG-ODN (sequence TCCATGACGTTCCTGACGTT, IDT, 10 mg/ml working solution in dH_2O) for 6–8 hours at RT and subsequently lyophilized. 2mg of the MSR (50mg/ml working solution in PBS) were adsorbed with various doses (indicated in figure legends) of linear or branched PEI (in 100ul PBS, pH to 7.4) at 37°C for 15 minutes (MSR-PEI particles), and various doses of antigen (typically 100ug OVA or 50ug peptides) were adsorbed onto MSR-PEI particles for 1–3 hours at 37 °C under shaking and subsequently lyophilized. Separately, 1mg of the MSRs (50mg/ml working solution in PBS) were loaded with 1ug murine GM-CSF (Peprotech, 1 mg/ml working solution) for 1 hour at 37°C under shaking. The MSR components (5mg total) were combined and resuspended in cold PBS (150ul per vaccine) prior to immunization.

To formulate the trans MSR-PEI vaccines, 2mg of the MSR (50mg/ml working solution in PBS) were adsorbed with various doses of antigens (typically 100ug OVA or 50ug peptides) for 6–8 hours at RT and subsequently lyophilized. 2mg of the MSR (50mg/ml working solution in PBS) were adsorbed with various doses (indicated in figure legends) of linear or branched PEI (in 100ul PBS, pH to 7.4) at 37 °C for 15 minutes (MSR-PEI particles), and adsorbed with 100ug murine class B CpG-ODN (sequence TCCATGACGTTCCTGACGTT, IDT, 10 mg/ml working solution in dH_2O) was adsorbed onto MSR-PEI particles for 1 hour at 37 °C under shaking. Separately, 1mg of the MSRs (50mg/ml working solution in PBS) were loaded with 1ug murine GM-CSF (Peprotech) for 1 hour at 37 °C under shaking. The MSR components (5mg total) were combined and resuspended in cold PBS (150ul per vaccine) prior to immunization.

To prepare the MSR vaccines, 4mg of the MSR (50mg/ml working solution in PBS)were adsorbed with 100ug murine class B CpG-ODN (sequence TCCATGACGTTCCTGACGTT, IDT, 10 mg/ml working solution in dH_2O) and the antigen (typically 100ug OVA or 50ug peptides) for 6–8 hours at room temperature under shaking, and subsequently lyophilized. Separately, 1mg of the MSRs (50mg/ml working solution in PBS) were loaded with 1ug murine GM-CSF (Peprotech) for 1 hour at 37 °C under shaking. The MSR components were combined and resuspended in cold PBS (150ul per vaccine) prior to immunization.

To prepare the bolus vaccine, 100ug murine class B CpG-ODN (sequence TCCATGACGTTCCTGACGTT, IDT, 10 mg/ml working solution in dH_2O), 1ug murine GM-CSF and the antigen (typically 50ug peptides) were combined in 150ul cold PBS.

Vaccine components were tested to be endotoxin free (Charles River Laboratories) (Supplementary Table 2).

Animals

C57BL/6J and Balb/c mice were purchased from Jackson Laboratories and housed at Harvard University. Female mice between 6 weeks and 10 weeks old at the start of the experiments were used. All studies were performed in accordance with institutional guidelines approved by Harvard University's Institutional Animal Care and Use Committee (IACUC)[31].

Immunization

MSR vaccines were resuspended in 150ul of cold PBS immediately before injection. They were injected, via an 18G needle, subcutaneously in the intrascapular region with the mouse under brief isoflurane anesthesia.

Pore measurement

MSRs and MSR-PEI particles were first lyophilized. Nitrogen sorption isotherms of the particles were measured at 77K using the ASAP 2000 system (Micromeritics). To determine the surface area of the particles, the Brunauer-Emmett-Teller (BET) method was used. To determine the pore size distributions, the Barret–Joyner–Hallenda (BJH) model from the adsorption branch of the isotherm was used[31].

Transmission electron microscopy (TEM)

To prepare the samples for TEM imaging, MSR and MSR-PEI particles were first diluted in 200-proof ethanol (Sigma Aldrich) to ~0.1 mg/ml and briefly sonicated. 5–20ul of the diluted particles was dripped onto Formvar/Carbon TEM grids (Ted Pella) and dried at room temperature. The particles were imaged using the JEOL 2100 Transmission Electron Microscope[31].

Endotoxin measurement

Analyzed samples without dilution were analyzed using EndoSafe cartridge kits (Charles River Laboratories, Cat #PTS55005F). Samples were assayed according to manufacturer protocols. Briefly, 25 ul of sample was added to samples and control wells and the assay was run on an EndoSafe, Multi-Cartridge System (Charles River Laboratories).

Incorporation efficiency assays

To determine the incorporation efficiency of peptides onto the MSRs, 50ug of the indicated peptides was adsorbed onto 2mg of MSRs or MSR-PEI particles overnight. The MSRs were centrifuged at 2000g for 10 min to separate the unbound peptides from the bound peptides. Supernatant containing the unbound peptides was collected and the concentration of the

peptides was quantified using micro-BCA (ThermoScientific). Quantification of peptide incorporation was confirmed using HPLC LC-MS (Supplementary Fig 13a). Incorporation efficiency was calculated as the total added to MSR minus the unbound portion. To ensure the accuracy of this approach, the bound peptides were dissociated from the MSRs with 40% Tween-20 under vigorous shaking for 4 hours at RT. Subsequently, the concentration of the peptides in the bound portion and the unbound portion was measured using LC-MS, and confirmed that nearly 100% of the peptides initially introduced to the particles were accounted for (Supplementary Fig 13b).

To determine the incorporation efficiency of PEI onto the MSRs, PEI at the indicated doses was adsorbed onto MSR for 15 min at 37 °C. Subsequently, the MSRs were centrifuged at 2000g for 10 min to separate the bound PEI from the unbound PEI. Supernatant was collected and the concentration of PEI was measured using Fluoraldehyde (Sigma Aldrich). Incorporation efficiency was calculated as the total minus the unbound portion.

In vitro release studies

2mg of MSRs were loaded with either 2ug of GM-CSF, 100ug of CpG, or 10ug of Rhodamine-PEI (L25K). The individual vaccine components were then resuspended in 1ml of release media, which is composed of RPMI (Sigma-Aldrich) supplemented with 1% penicillin/ streptomycin and 10% heat-inactivated FBS (Sigma-Aldrich), in low-binding Eppendorf tubes. Release study was then performed in 37 °C under gentle shaking. Periodically, supernatant containing the released component was collected by pelleting the particles at 2000g for 10 min. The release media was subsequently replaced. For analysis, GM-CSF content was determined using ELISA (R&D). CpG content was detected using OliGreen (ThermoFisher)[13].

BMDC differentiation, cytokine production and antigen presentation assays

DCs were differentiated from bone marrow cells isolated from C57Bl/6J mice (Jackson Laboratories). Bone marrow was collected from the femur and tibiae bone, and single cell suspensions were cultured in RPMI (Sigma Aldrich) supplemented with 10% heat inactivated FBS (Sigma-Aldrich), 1% penicillin/streptomycin, 50μM β-mercaptoethanol and 20 ng/ml murine GM-CSF (Peprotech). Non-adherent and loosely-adherent cells between days 7 and 10 of differentiation were collected and used for the studies. Differentiation was confirmed by staining the cells with anti-mouse CD11c and CD11b. To assess the uptake kinetics of PEI by BMDCs, 0.5×10^6/ml immature BMDCs were plated onto non-tissue culture treated 12-well dishes and stimulated with 7ug of rhodamine labeled L25K PEI for various time lengths (0h, 2h, 6h, 24h, 72h). BMDCs were harvested, resuspended in FACS buffer and the rhodamine signal was analyzed using flow cytometry (BD Biosciences). To assess the BMDCs activity after PEI stimulation, 1×10^6/ml immature BMDCs were plated onto tissue culture treated 12-well dishes and stimulated with various doses of L25K or B60K PEI or MSR-PEI for 24 hours, either in the presence or absence of 20ng/ml LPS. BMDCs were harvested, resuspended in FACS buffer and stained with 7-AAD (eBioscience), anti-CD11c, anti-CD86 and anti-MHCII for 15 minutes on ice. BMDCs were then washed in FACS buffer and analyzed using flow cytometry. Separately, supernatant was collected and analyzed for IL-1β, IL-6, TNFα and IFNγ using ELISA according to the

manufacturer's protocols (eBioscience). To assess BMDC cross presentation, 0.5×10^6/ml BMDCs were pulsed with 20ug ovalbumin (Invivogen) either alone or in the presence of 5ug or 10 B60K PEI for 48 hours. BMDCs were then harvested and stained using 7-AAD (Biolegend), anti-CD11c and anti-SIINFEKL/H-2Kb for 15 min. on ice, washed and analyzed using flow cytometry (LSRFortessa, BD)[32].

Lysosomal rupture in BMDCs

1×10^6/ml immature BMDCs were plated onto tissue culture treated 12-well dishes. BMDCs were stimulated with 40ug of MSR, 40ug of MSR-PEI particles (12.5ug of L25K-PEI/mg MSR) or 2ug free PEI (L25K) for 24 hours. Subsequently, BMDCs were incubated with acridine orange (ThermoFisher, diluted 1:20,000) for 4 hours. Acridine orange signal was assessed using flow cytometry at 488 nm (excitation) and 650–690 nm (emission) (LSRFortessa, BD)[21].

TLR-4 neutralization

1×10^6/ml immature BMDCs were plated onto tissue culture treated 12-well dishes and treated with TLR4 (CD284)/MD2 monoclonal antibody (Biolegend, clone MTS510) for 1 hour at 37 °C. Subsequently, the BMDCs were stimulated with 40ug of MSR or MSR-PEI particles (12.5ug PEI/mg MSR) for 24 hours. BMDCs were collected, stained with anti-CD11c, anti-CD86 and 7AAD, and analyzed using flow cytometry (LSRFortessa, BD).

Therapeutic tumor studies

Cells were used at passage number <5 and passaged at least twice prior to inoculation. In the subcutaneous therapeutic TC-1 model, female C57BL/6 mice were injected with a single cell suspension of 2×10^5 TC-1 cells in 100ul cold PBS on the back of the neck on day 0. In the subcutaneous therapeutic B16F10 model, female C57BL/6 mice were injected with a single cell suspension of 1×10^5 B16F10 cells in 100ul cold PBS on the back of the neck on day 0. Mice were immunized on indicated days, and tumor area was monitored using a caliper: longest surface length (a) and width (b), and the tumor size was expressed as area (a×b). Mice were euthanized when the largest side reached 2cm or according to IACUC standards. In the therapeutic B16F10 or CT26 lung metastasis model, mice were injected intravenously with 2×10^5 B16F10 or CT26 cells in 100ul cold PBS on day 0. Lungs were excised on day 16 and fixed in Fekete's solution. Lung metastasis nodules were then manually enumerated. For anti-CTLA4 therapies, 100ug per mouse of anti-mouse CTLA-4 antibodies (BioXcell, clone: 9D9) were administered intraperitoneally on days 1, 3, 6 and 9 after tumor inoculation.

$CD8^+$ T cell depletion

$CD8^+$ T cells were depleted by injecting 100ug of anti-CD8a monoclonal antibody (BioXCell, clone 2.43) intraperitoneally twice weekly, starting the day before vaccination[33]. Depletion was confirmed using flow cytometry.

Scaffold explant and analysis

Scaffold tissues were surgically removed from the animals after euthanasia. They were first processed using mechanical disruption, and subsequently digested in 250 U/ml Collagenase IV (Worthington) in RPMI for 30 min. at 37 °C under gentle shaking. Cell and tissue suspensions were filtered through a 40μm cell strainer to separate single cells from large MSR particles. The cells and small remaining MSR particles were pelleted, washed three times, and counted manually using a hemacytometer. Dead cells were visualized using Trypan Blue (ThermoFisher). Subsequently, cells were stained with anti-mouse CD11c, CD86, CCR7 and SIINFEKL/H-2K^b monoclonal antibodies in FACS buffer (PBS supplemented with 1% BSA and 0.1% sodium azide) for 15 min. on ice. Dead cells and MSR particles were stained and excluded from analysis using 7-AAD (eBioscience) or a fixable viability dye (eBioscience). Finally, cells were washed 3 times in FACS buffer and analyzed using flow cytometry (LSRFortessa, BD)[13].

Lymph node analysis

Vaccine draining lymph nodes were surgically removed from the animals. They were then processed through mechanical disruption and digested for 30 min. at 37 °C in RPMI containing 0.5mg/ml Collagenase 4 and 0.1 mg/ml DNAse. Cells were then filtered through a 40μm cell and washed in cold PBS. Single cell suspensions were enumerated (Beckman-Coulter) and stained with a alexa-fluor 780 dead exclusion dye (eBioscience), anti-mouse CD11c, CD11b, CD86, MHC-II and F4/80 for 15 min. on ice. DQ-OVA was visualized in the FITC channel. The cells were then washed and analyzed using flow cytometry (LSRFortessa, BD).

Tetramer analysis and peptide restimulation of circulating PBMCs

~100ul of periphery blood was collected into heparin coated tubes (BD) and kept on ice. Red blood cells (RBCs) were removed by adding 1ml RBC lysis buffer (BioLegend) for 1 min. at RT; lysis was quenched by adding 9 ml cold PBS directly. Cells were pelleted and washed in FACS staining buffer. To perform tetramer staining, blood cells were incubated with 50ul of 7ug/ml alexa fluor 647 conjugated peptide-MHC tetramers (NIH Tetramer Core) for 20 min. at 37 °C. Subsequently, cells were pelleted and stained with 7-AAD, anti-mouse CD3e and CD8a for 15 min. on ice. Finally, cells were washed three times in FACS staining buffer and analyzed using flow cytometry (LSRFortessa). To perform peptide restimulation, blood cells were pulsed with 2ug/ml of various MHC-I restricted peptides for 1–1.5 hours at 37 °C in T cell media (RPMI supplemented with 110mg/L sodium pyruvate, 5mM HEPES, 50 μM β-mercaptoethanol, 10% heat inactivated FBS and 1% penicillin/streptomycin). Subsequently, cytokine secretion was stopped by directly adding Golgi Plug (Biolegend) to the culture. Cells were cultured for another 4 hours at 37 °C. Cells were pelleted and stained with Alexa-Fluor 780 dead exclusion dye, anti-mouse CD3e, CD8a and CD4 for 15 min. on ice. Cells were then fixed and permeablized (eBioscience 88-8824-00), and stained with anti-mouse IFNγ for 30 min. in 4 °C. Finally, cells were washed and analyzed using flow cytometry (LSRFortessa, BD).

Peptide restimulation of splenic CD8+ T cells

To isolate splenic DCs, naïve spleens were retrieved and digested in RPMI supplemented with 1 mg/ml collagenase 4 (Worthington) and 0.1 mg/ml DNase (New England Biolabs) for 30 minutes in 37 °C. RBCs were lysed using RBC lysis buffer (Biolgend). Dead cells were removed (Miltenyi Biotec), and splenic DCs were obtained using a $CD11c^+$ magnetic sorting kit (Miltenyi Biotec). DCs were pulsed with 5 ug/ml of the M27, M30, or a control peptide. Separately, spleens from vaccinated mice were retrieved (8 days after vaccination). Splenocytes were isolated from the spleens by physically grinding the spleens on a cell filtration device in RPMI supplemented with 2% FBS. RBCs were lysed and $CD8^+$ or $CD4^+$ T cells were then obtained using a negative $CD8^+$ or $CD4^+$ T cell selection kit (Miltenyi Biotec). The sorted T cells were labeled with CFSE (ThermoFisher). T cells and DCs were cultured together at a 10:1 (T:DC) ratio for 3 days at 37 °C to allow for antigen-specific T cell proliferation. On day 3, cytokine secretion was stopped by incubating with golgi plug (Biolegend) for 4 hours at 37 °C. Subsequently, cells were collected and stained with Alexa-Fluor 780 dead exclusion dye, anti-mouse CD3e, CD8a and CD4 for 15 min on ice before fixing and permeabilizing (eBioscience 88-8824-00). Cells were then stained with anti-mouse IFNγ for 30 min. in 4 °C and analyzed using flow cytometry (LSRFortessa, BD)[5,34].

Tumor infiltrating lymphocyte (TIL) analysis

Tumors were explanted and cut into small pieces in 5ml of RPM. The samples were then digested in 15ml RPMI supplemented with 2% FCS, 50U/ml Collagenase IV (Invitrogen), 100ug/ml Hyaluronidase and 20U/ml DNase (Roche) for 2 hours at 37 °C using the gentleMACS Dissociators (Miltenyi Biotech). Suspensions were filtered through a 40μM strainer and washed 3× with PBS. Lymphocyte population was enriched through gradient centrifugation at 50g for 5 minutes and repeated 3 times. Supernatant was collected and stained with a Zombie-UV dead exclusion dye, anti-mouse CD45, CD3e, CD4, CD8a, CD62L and CD44 for 15 min. on ice before fixing and permeablizing (eBioscience 00-5523-00). Cells were then stained with anti-mouse IFNγ, TNFα and Granzyme B for 30 min. in 4 °C and analyzed using flow cytometry (LSRFortessa, BD)[35].

Statistical analysis

All values in the present study were expressed as mean ± S.D unless otherwise indicated in the figure legends. Statistical analysis was performed using GraphPad Prism. The significance between two groups was analyzed by a, two-tailed, student's t test. Sample variance was tested using the F test. For multiple comparisons, a one-way or a two-way ANOVA test was used. In all cases, a P-value of less than 0.05 was considered significant. Details for statistical analyses for each comparison are reported in Supplementary Table 6.

Supplementary Material

Refer to Web version on PubMed Central for supplementary material.

Acknowledgments

The authors would like to thank Dr. Catherine J. Wu (Dana Farber Cancer Institute) for providing the human neoantigen peptides. We are also grateful to Dr. Glenn Dranoff, Dr. Catia S. Verbeke, Dr. George J. Xu and Dr. Alex

S. Cheung for their helpful discussions and feedback on the manuscript. This work was supported by the National Institutes of Health (NIH) R01EB015498, the Melanoma Research Alliance Foundation, the National Science Foundation (NSF) Graduate Research Fellowship Program (AWL) and the Wyss Institute for Biologically Inspired Engineering.

References

1. Gubin MM, Artyomov MN, Mardis ER, Schreiber RD. Tumor neoantigens: building a framework for personalized cancer immunotherapy. The Journal of clinical investigation. 2015; 125:3413–3421. [PubMed: 26258412]
2. Schumacher TN, Schreiber RD. Neoantigens in cancer immunotherapy. Science. 2015; 348:69–74. [PubMed: 25838375]
3. Hacohen N, Fritsch EF, Carter TA, Lander ES, Wu CJ. Getting personal with neoantigen-based therapeutic cancer vaccines. Cancer immunology research. 2013; 1:11–15. [PubMed: 24777245]
4. Linnemann C, et al. High-throughput epitope discovery reveals frequent recognition of neo-antigens by CD4+ T cells in human melanoma. Nature medicine. 2015; 21:81–85.
5. Kreiter S, et al. Mutant MHC class II epitopes drive therapeutic immune responses to cancer. Nature. 2015; 520:692–696. [PubMed: 25901682]
6. Ott PA, et al. An immunogenic personal neoantigen vaccine for patients with melanoma. Nature. 2017; 547:217–221. [PubMed: 28678778]
7. van der Burg SH, Arens R, Ossendorp F, van Hall T, Melief CJ. Vaccines for established cancer: overcoming the challenges posed by immune evasion. Nature Reviews Cancer. 2016; 16:219–233. [PubMed: 26965076]
8. Moon JJ, et al. Interbilayer-crosslinked multilamellar vesicles as synthetic vaccines for potent humoral and cellular immune responses. Nat Mater. 2011; 10:243–251. DOI: 10.1038/nmat2960 [PubMed: 21336265]
9. Liu H, et al. Structure-based programming of lymph-node targeting in molecular vaccines. Nature. 2014; 507:519–522. DOI: 10.1038/nature12978 [PubMed: 24531764]
10. Cho NH, et al. A multifunctional core-shell nanoparticle for dendritic cell-based cancer immunotherapy. Nat Nanotechnol. 2011; 6:675–682. DOI: 10.1038/nnano.2011.149 [PubMed: 21909083]
11. Cho HJ, et al. Immunostimulatory DNA-based vaccines induce cytotoxic lymphocyte activity by a T-helper cell-independent mechanism. Nature biotechnology. 2000; 18:509–514.
12. Bobisse S, Foukas PG, Coukos G, Harari A. Neoantigen-based cancer immunotherapy. Annals of Translational Medicine. 2016; 4
13. Kim J, et al. Injectable, spontaneously assembling, inorganic scaffolds modulate immune cells in vivo and increase vaccine efficacy. Nat Biotech. 2015; 33:64–72. DOI: 10.1038/nbt.3071
14. Song WJ, Du JZ, Sun TM, Zhang PZ, Wang J. Gold nanoparticles capped with polyethyleneimine for enhanced siRNA delivery. Small. 2010; 6:239–246. [PubMed: 19924738]
15. Sakai S, Yamada Y, Yamaguchi T, Ciach T, Kawakami K. Surface immobilization of poly(ethyleneimine) and plasmid DNA on electrospun poly(L-lactic acid) fibrous mats using a layer-by-layer approach for gene delivery. J Biomed Mater Res A. 2009; 88:281–287. DOI: 10.1002/jbm.a.31870 [PubMed: 18260146]
16. Oh Y-K, et al. Enhanced adjuvanticity of interleukin-2 plasmid DNA administered in polyethylenimine complexes. Vaccine. 2003; 21:2837–2843. [PubMed: 12798625]
17. Mulens-Arias V, Rojas JM, Pérez-Yagüe S, Morales MP, Barber DF. Polyethylenimine-coated SPIONs trigger macrophage activation through TLR-4 signaling and ROS production and modulate podosome dynamics. Biomaterials. 2015; 52:494–506. [PubMed: 25818455]
18. Wegmann F, et al. Polyethyleneimine is a potent mucosal adjuvant for viral glycoprotein antigens. Nature biotechnology. 2012; 30:883–888.
19. Sheppard NC, et al. Polyethyleneimine is a potent systemic adjuvant for glycoprotein antigens. International immunology. 2014; 26:531–538. [PubMed: 24844701]
20. He W, et al. Re-polarizing myeloid-derived suppressor cells (MDSCs) with cationic polymers for cancer immunotherapy. Scientific reports. 2016; 6

21. Hornung V, et al. Silica crystals and aluminum salts activate the NALP3 inflammasome through phagosomal destabilization. Nat Immunol. 2008; 9:847–856. DOI: 10.1038/ni.1631 [PubMed: 18604214]
22. Eisenbarth SC, Colegio OR, O'Connor W, Sutterwala FS, Flavell RA. Crucial role for the Nalp3 inflammasome in the immunostimulatory properties of aluminium adjuvants. Nature. 2008; 453:1122–1126. DOI: 10.1038/nature06939 [PubMed: 18496530]
23. Vollmer J, Krieg AM. Immunotherapeutic applications of CpG oligodeoxynucleotide TLR9 agonists. Advanced drug delivery reviews. 2009; 61:195–204. [PubMed: 19211030]
24. Bartkowiak T, et al. Unique potential of 4-1BB agonist antibody to promote durable regression of HPV+ tumors when combined with an E6/E7 peptide vaccine. Proceedings of the National Academy of Sciences. 2015; 112:E5290–E5299.
25. Chaturvedi AK. Beyond cervical cancer: burden of other HPV-related cancers among men and women. Journal of Adolescent Health. 2010; 46:S20–S26. [PubMed: 20307840]
26. Welters MJ, et al. Vaccination during myeloid cell depletion by cancer chemotherapy fosters robust T cell responses. Science translational medicine. 2016; 8:334ra352–334ra352.
27. Zwaveling S, et al. Established human papillomavirus type 16-expressing tumors are effectively eradicated following vaccination with long peptides. The Journal of Immunology. 2002; 169:350–358. [PubMed: 12077264]
28. van der Sluis TC, et al. Therapeutic peptide vaccine-induced CD8 T cells strongly modulate intratumoral macrophages required for tumor regression. Cancer immunology research. 2015; 3:1042–1051. [PubMed: 25888578]
29. Kranz LM, et al. Systemic RNA delivery to dendritic cells exploits antiviral defence for cancer immunotherapy. Nature. 2016
30. Kvistborg P, et al. Anti-CTLA-4 therapy broadens the melanoma-reactive CD8+ T cell response. Sci Transl Med. 2014; 6:254ra128.
31. Li WA, et al. The effect of surface modification of mesoporous silica micro-rod scaffold on immune cell activation and infiltration. Biomaterials. 2016; 83:249–256. [PubMed: 26784009]
32. Kim J, et al. Effect of pore structure of macroporous poly (lactide-co-glycolide) scaffolds on the in vivo enrichment of dendritic cells. ACS applied materials & interfaces. 2014; 6:8505–8512. [PubMed: 24844318]
33. Moynihan KD, et al. Eradication of large established tumors in mice by combination immunotherapy that engages innate and adaptive immune responses. Nature medicine. 2016; 22(12):1402–1410.
34. Höpken UE, et al. The ratio between dendritic cells and T cells determines the outcome of their encounter: proliferation versus deletion. European journal of immunology. 2005; 35:2851–2863. [PubMed: 16180253]
35. Zhou P, et al. In vivo Discovery of Immunotherapy Targets in the Tumor Microenvironment. Nature. 2014; 506:52. [PubMed: 24476824]

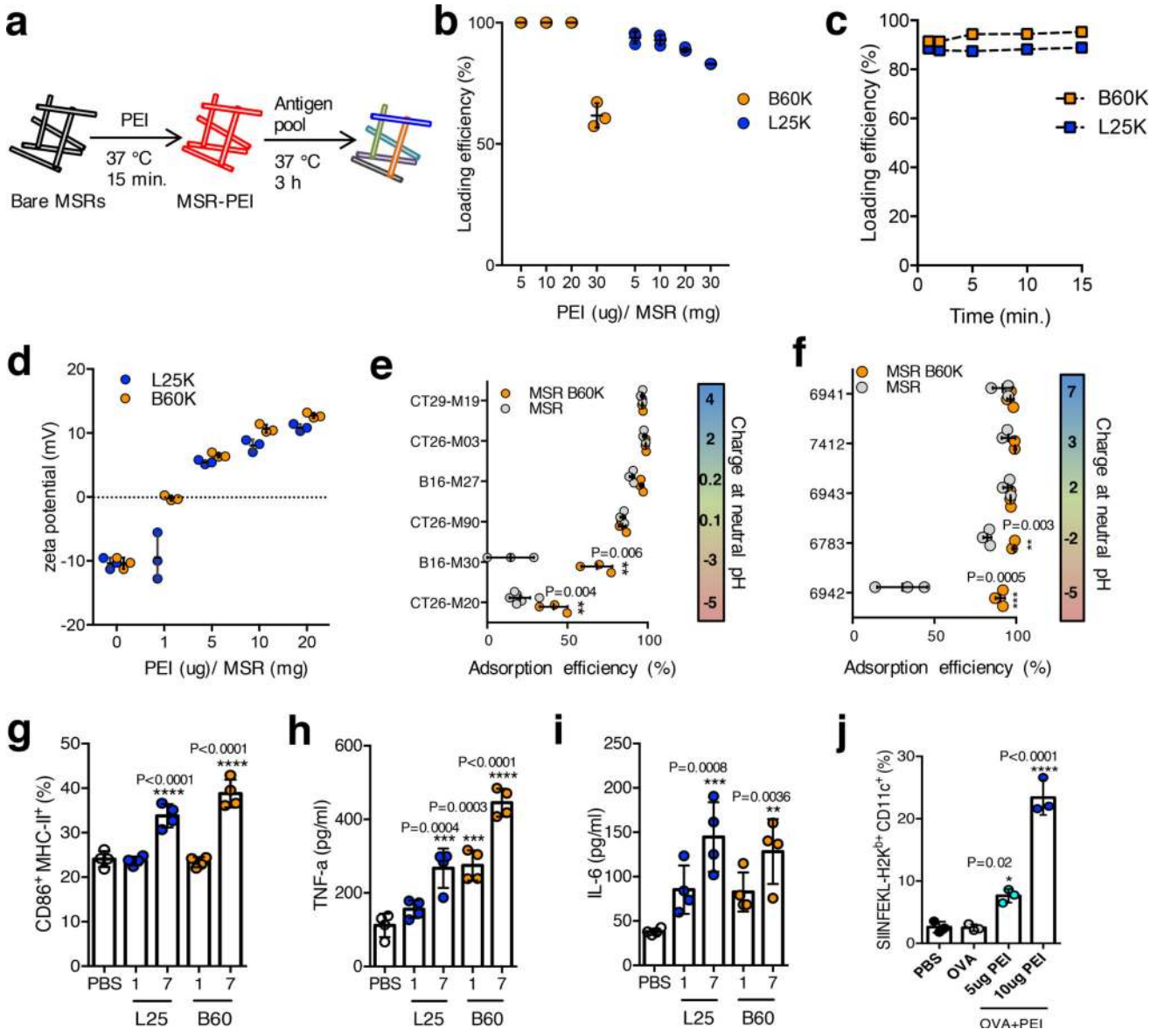

Figure 1. PEI can be rapidly incorporated onto MSRs and leads to murine and human DC activation

(a) Schematics of PEI and subsequent antigen adsorption onto bare MSRs. (b) Incorporation efficiency of various doses of soluble B60K and L25K PEI into MSRs (n=3). (c) Incorporation kinetics of soluble B60K and L25K PEI into MSRs (representative data, repeated at least 3 times). (d) Zeta potential of MSR-PEI particles using various doses of soluble B60K and L25K PEI (n=3). Incorporation efficiency of (e) murine and (f) human neoantigen peptides (sorted according to the net charge at neutral pH) onto bare MSR or MSR-PEI particles using B60K PEI (n=3, two-tailed T test). (g) Flow cytometry analysis of CD86 and MHC-II expression on murine BMDCs after 24 hours of stimulation with 1ug or 7ug of soluble PEI or PBS (n=4, compared to PBS by one-way ANOVA). ELISA analysis of (h) TNFα and (i) IL-6 concentration in murine BMDC supernatant after 24 hours of stimulation with 1ug or 7ug of soluble B60K and L25K PEI or PBS (n=4, compared to PBS

by one-way ANOVA). (j) Flow cytometry analysis of SIINFEKL presenting murine BMDCs after stimulation with PBS, OVA and OVA with 5ug or 10ug of soluble B60K PEI (n=3, compared to OVA by one-way ANOVA). Data depicts mean +/− sd.

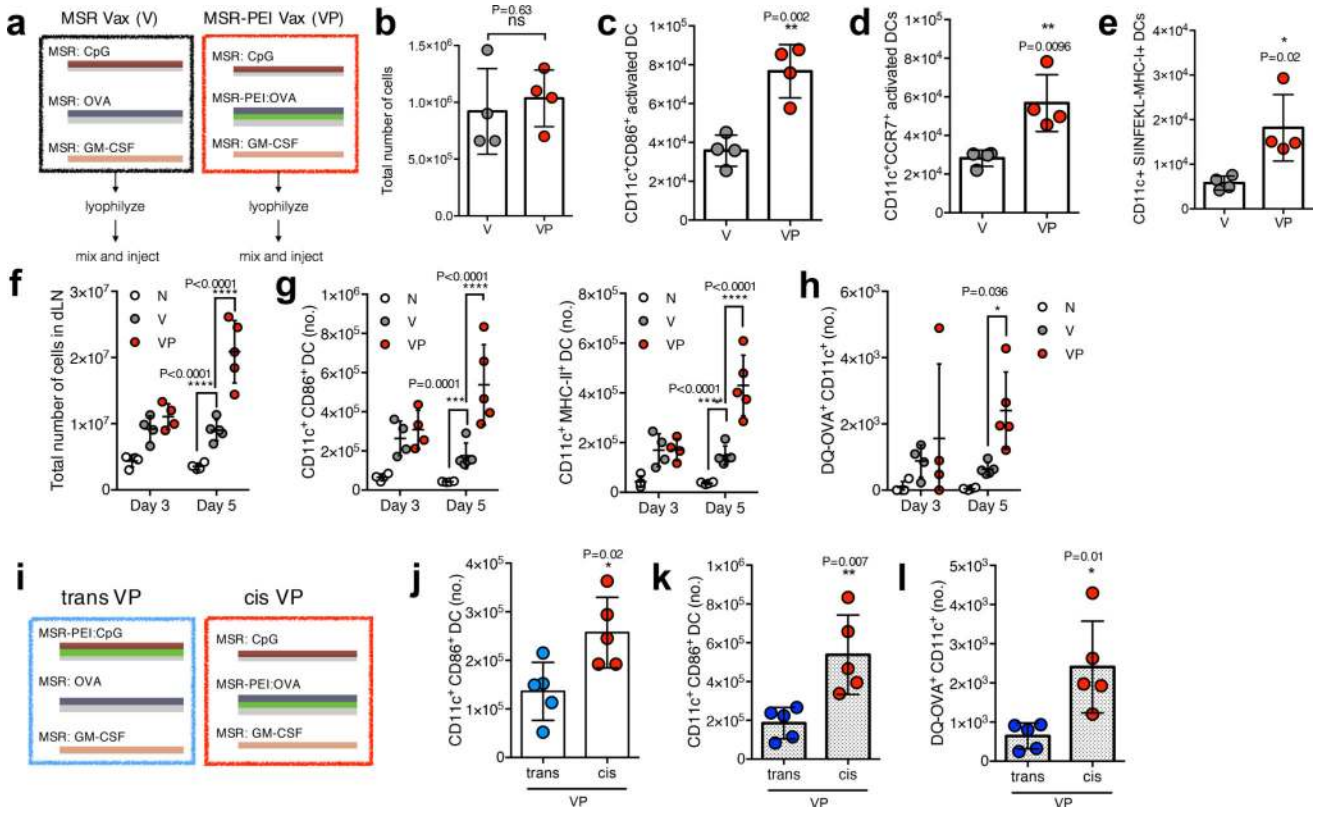

Figure 2. MSR-PEI vaccine enhances DC activation and trafficking in situ

(a) Schematics of the MSR vaccine (V) and MSR-PEI vaccine (VP). (b) Total cell number at the vaccine site explanted on day 3 post immunization with the MSR vaccine (V), the MSR-PEI vaccine (VP) using B60K PEI (n=4, two-tailed T test). Total number of (c) $CD11c^+$ $CD86^+$ activated DCs (n=4, two-tailed T test), (d) $CD11c^+$ $CCR7^+$ LN homing DCs (n=4, two-tailed T test) and (e) SIINFEKL presenting DC (n=4, two-tailed T test) recruited to the vaccine site on day 3 post immunization with the MSR vaccine (V), the MSR-PEI vaccine (VP) using B60K PEI. (f) Total number of cells (n=4 for d3 and n=5 for d5, two-way ANOVA), of (g) $CD11c^+$ $CD86^+$ or $CD11c^+$ $MHC\text{-}II^+$ activated DCs (n=4 for d3 and n=5 for d5, two-way ANOVA), and (h) OVA^+ DC (n=4 for d3 and n=5 for d5, two-way ANOVA) in the dLN on days 3 and day 5 post immunization with the MSR vaccine (V), the MSR-PEI vaccine (VP) using B60K PEI or left unimmunized (N). (i) Schematics of the MSR-PEI trans vaccine (trans VP) and the MSR-PEI cis vaccine (cis VP). (j) Total number of $CD11c^+$ $CD86^+$ activated DCs at the vaccine site on day 3 post immunization with the trans VP vaccine or the cis VP vaccine (n=5, two-tailed T test). Total number of (k) $CD11c^+$ $CD86^+$ activated DCs and (l) $CD11c^+$ OVA^+ DCs in the dLN on day 5 post immunization with the trans VP vaccine or the cis VP vaccine (n=5, two-tailed T test). Data depicts mean +/− sd

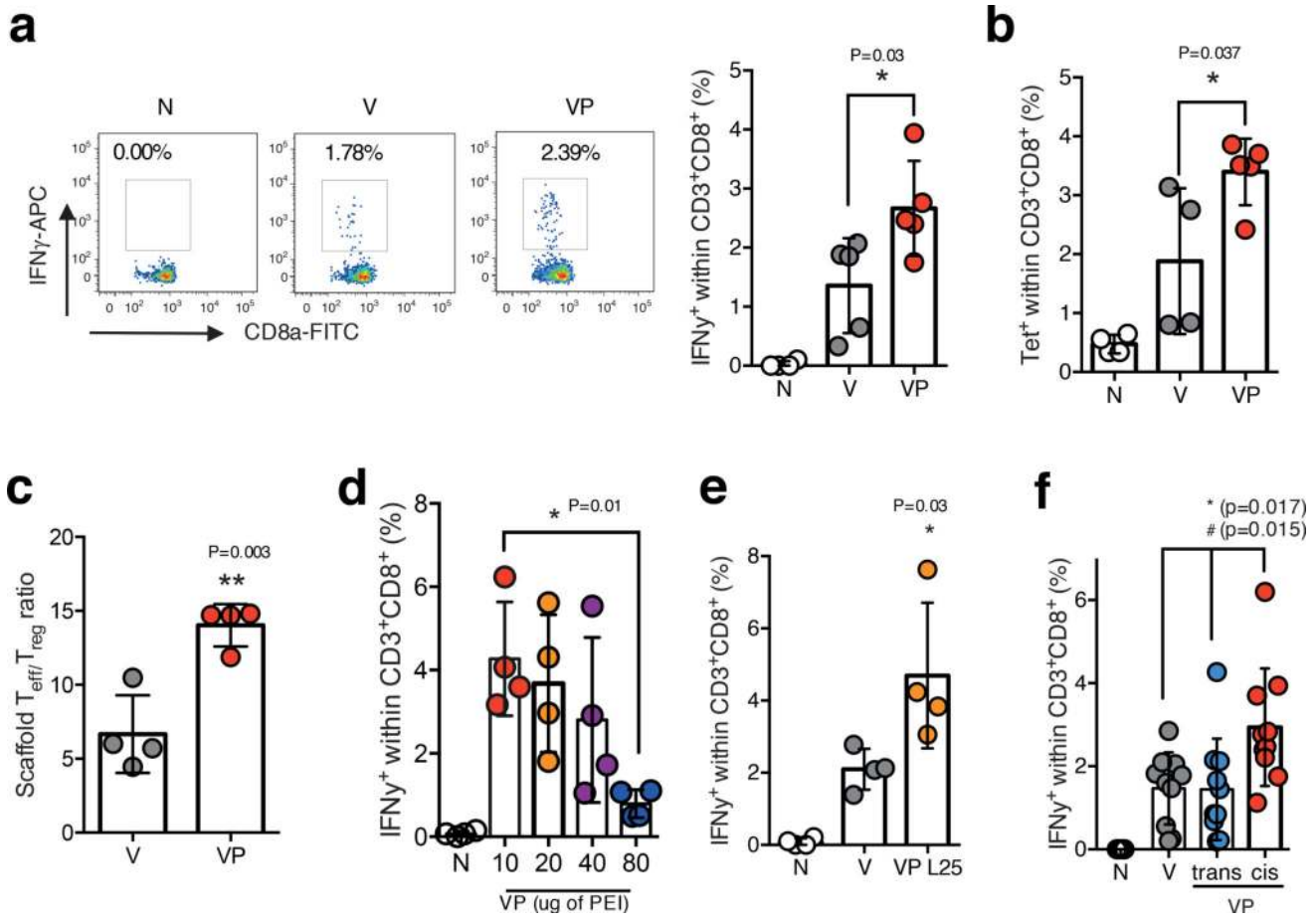

Figure 3. MSR-PEI vaccine enhances CD8 cytotoxic T cell response against OVA

(a) Percentage of IFNγ^+ CD8$^+$ T cells isolated from peripheral blood on day 7 after immunization with the MSR vaccine (V), the MSR-PEI vaccine (VP) using B60K PEI, or left unimmunized (N), and stimulated with SIINFEKL (primary FACS plots on the left, quantifications from the FACS plots on the right) (n=5, one-way ANOVA). (b) Percentage of SIINFEKL-tetramer$^+$ CD8$^+$ T cells isolated from peripheral blood on day 7 after immunization with the MSR vaccine (V), the MSR-PEI vaccine (VP) using B60K PEI or left unimmunized (N) (n=5 for VP, n=4 for N and V, one-way ANOVA). (c) Ratio of CD8$^+$ effector T cells (Teff) to CD4$^+$ Foxp3$^+$ regulatory T cells (Treg) at the MSR vaccine site on day 11 after immunization with the MSR vaccine (V) or the MSR-PEI vaccine (VP) using B60K PEI (n=5, two-tailed T test). (d) Percentage of IFNγ^+CD8$^+$ T cells isolated from peripheral blood on day 7 after immunization with the MSR-PEI vaccine (VP) containing various doses of B60K PEI or left unimmunized (N) (n=4, one-way ANOVA). (e) Percentage of IFNγ^+CD8$^+$ T cells isolated from peripheral blood at day 7 after immunization with the MSR vaccine (V), the MSR-PEI vaccine using L25K PEI (VP L25) or left unimmunized (N) (n=4, one-way ANOVA). (f) Percentage of IFNγ^+CD8$^+$ T cells isolated from peripheral blood at day 7 after immunization with the MSR vaccine (V), the MSR-PEI trans vaccine (trans, VP) using B60K PEI, and the MSR-PEI cis vaccine (cis, VP) using B60K PEI, or left unimmunized (N) and stimulated with SIINFEKL (n=9, * between

cis VP and trans VP, # between cis VP and V by one-way ANOVA). Data depicts mean +/− sd.

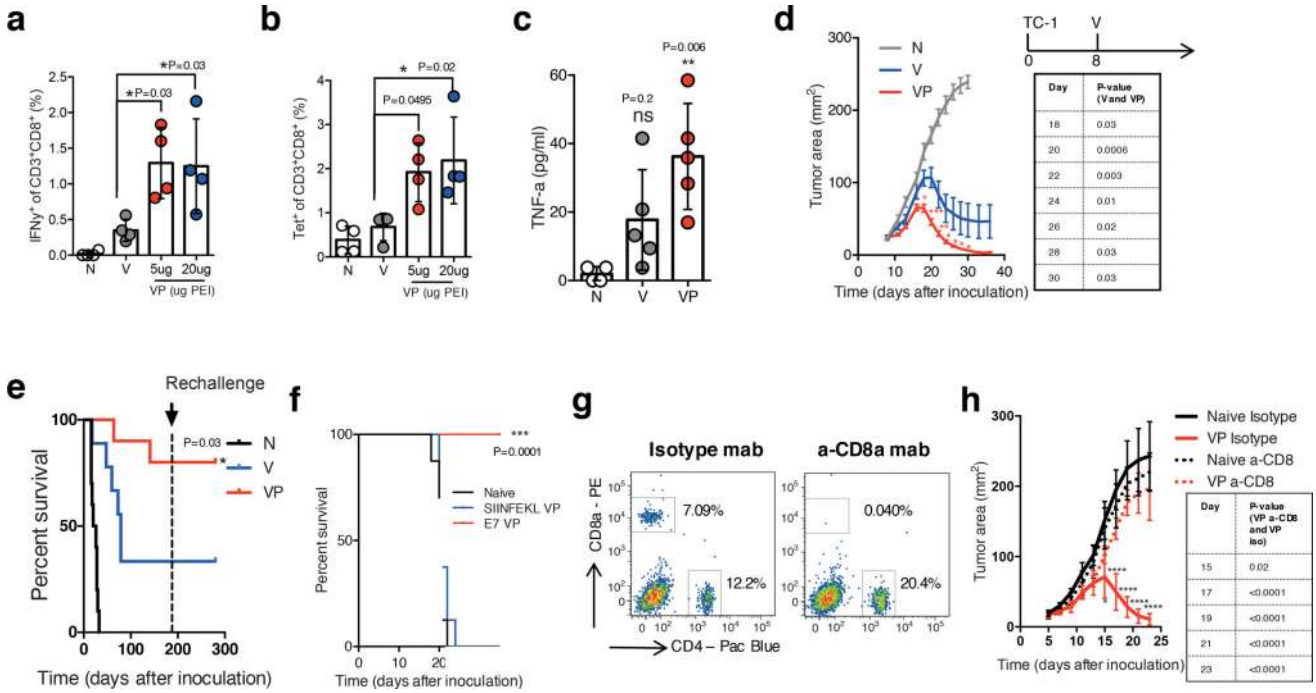

Figure 4. MSR-PEI vaccine enhances CD8 cytotoxic T cell response against E7 and regresses established tumors

(a) Percentage of IFNγ^+CD8$^+$ T cells in response to RAHYNIVTF stimulation and (b) percentage of tetramer$^+$CD8$^+$ T cells in peripheral blood on day 7 after immunization with the MSR E7 vaccine (V), the MSR-PEI E7 vaccine (VP) using 5ug or 20ug of B60K PEI, or left unimmunized (N) (n=4, one-way ANOVA). ELISA analysis of (c) TNFa level in serum 24 hours post vaccination with the MSR vaccine (V), the MSR-PEI (B60K) vaccine (VP), or left unimmunized (N) (n=4, compared to N by one-way ANOVA). (d) Tumor growth and (e) overall survival of mice bearing established E7 expressing TC-1 tumors (allowed to develop for 8 days) and treated with the MSR vaccine (V) or the MSR-PEI vaccine (VP) using L25K PEI, or left untreated (N), and subsequently rechallenged with TC-1 cells at 6 months post first inoculation (n=10, compared to V by two-way ANOVA for d, by Log-rank Test for e). (f) Overall survival of mice bearing established E7 expressing TC-1 tumors and treated with the MSR-PEI vaccine containing E7 (E7 VP) or the MSR-PEI vaccine containing SIINFEKL (SIINFEKL VP), or left untreated (Naive) (n=8, compared to SIINFEKL VP by Log-rank Test). (g) Flow cytometry analysis of blood T cells 3 days after treatment with a-CD8a mab or an isotype mab (representative data, repeated 3 times). (h) Tumor growth of mice bearing established E7 expressing TC-1 tumors and treated with the MSR-PEI vaccine with either a-CD8a mab or an isotype mab (n=8, compared to VP a-CD8 by two-way ANOVA). In (a–c), data depicts mean +/− sd and in (d,h), data depicts mean +/− sem

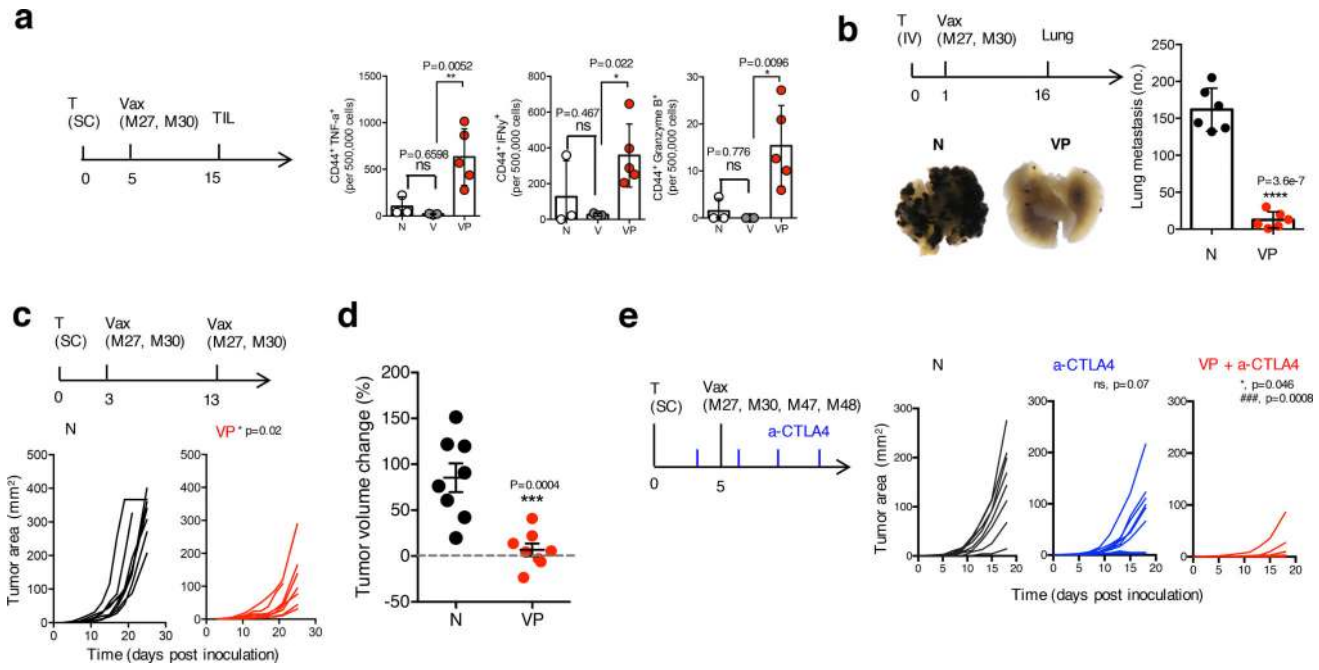

Figure 5. MSR-PEI vaccine enhances melanoma TIL effector function and induces tumor control and synergy with anti-CTLA4 therapy using combined B16 neoantigens

(a) Number of $CD44^+IFN\gamma^+$, $CD44^+TNF\alpha^+$ and $CD44^+$Granzyme B^+ TILs per 500,000 tumor cells on day 15 post inoculation. Mice bearing established B16F10 tumors (allowed to develop for 5 days) and treated with the MSR vaccine (V) or the MSR-PEI vaccine (VP) using L25K PEI and 50ug of the B16 neoantigens, or left untreated (N) (n=5 for VP, n=3 for N and V, one-way ANOVA). (b) Number of lung metastases formed on day 16 post inoculation in mice that received IV inoculation of B16F10 melanoma cells (allowed to develop for 1 day) and treated with the MSR-PEI vaccine (VP) using L25K PEI and 50ug of the B16 neoantigens, or left untreated (N). Primary representative photographs of excised lungs are shown in the figure (n=6, two-tailed T test). (c) Tumor growth in mice bearing established B16F10 tumors (allowed to develop for 3 days) and treated with two injections of the MSR-PEI vaccine (VP) using L25K PEI and 50ug of the B16 neoantigens on days 3 and 13, or left untreated (N) (n=8, two-tailed T test). (d) Tumor volume change between days 13 and 17 after tumor inoculation (n=8, two-tailed T test). (e) Tumor growth of mice bearing established B16F10 tumors (inoculated with 1×10^5 cells) and treated with anti-CTLA4 antibody (a-CTLA4), anti-CTLA4 antibody in combination with the MSR-PEI vaccine (VP+a-CTLA4) using L25K PEI and 50ug of the B16 neoantigens on days 5, or left untreated (N) (n=8, * between VP+a-CTLA4 and a-CTLA4, ### between VP+a-CTLA4, ns between a-CTLA4 and N by one-way ANOVA). In (a, b, d), data depicts mean +/− sd, in (c and e) data depicts individual tumor growth.